An impedimetric biosensor for the diagnosis of renal cell carcinoma based on the interaction between 3-aminophenyl boronic acid and sialic acid

Lei Zhang, Chao Yu, Rufei Gao, Yazhen Niu, Yuliang Li, Jun Chen, Junlin He

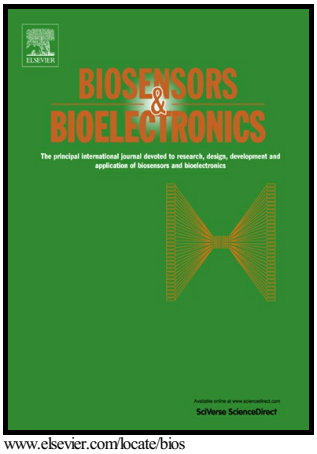

www.elsevier.com/locate/bios

PII: S0956-5663(16)31123-X
DOI: http://dx.doi.org/10.1016/j.bios.2016.10.083
Reference: BIOS9305

To appear in: *Biosensors and Bioelectronic*

Received date: 8 July 2016
Revised date: 27 October 2016
Accepted date: 28 October 2016

Cite this article as: Lei Zhang, Chao Yu, Rufei Gao, Yazhen Niu, Yuliang Li, Jun Chen and Junlin He, An impedimetric biosensor for the diagnosis of rena cell carcinoma based on the interaction between 3-aminophenyl boronic acid an sialic acid, *Biosensors and Bioelectronic* http://dx.doi.org/10.1016/j.bios.2016.10.083

An impedimetric biosensor for the diagnosis of renal cell carcinoma based on the interaction between 3-aminophenyl boronic acid and sialic acid

Lei Zhang[1], Chao Yu[1], Rufei Gao, Yazhen Niu, Yuliang Li, Jun Chen, Junlin He[*]

School of Public Health and Management, Institute of Life Science, Chongqing Medical University, Chongqing 400016, P. R. China

[*]Corresponding author: Prof. Junlin He, Full address: Box 197, Chongqing Medical University, No.1 Yixueyuan Road, Yuzhong District, Chongqing 400016, P. R. China. Tel: (86)23-68485926; Fax: (86) 23-68485008. Email: hejunlin_11@aliyun.com

ABSTRACT

Renal cell carcinoma (RCC) often expresses a high density of sialic acid-rich glycoproteins which helps these late-stage cancer cells to enter the blood stream or urine. Blood diagnosis is a complex and time-consuming process. In this study, we developed a facile and non-invasive electrochemical cytosensor for early detection of RCC in urine samples based on specific recognition by 3-aminophenyl boronic acid (APBA). Polypyrrole (PPy) and bovine serum albumin (BSA)-incorporated Ag submicron particles (Ag@BSA) were co-deposited on a gold electrode (GE) to take advantages of the excellent properties of these biomaterials, including good biocompatibility, low cytotoxicity and excellent electro-conductivity. To further increase the biosensor's sensitivity, APBA molecules were integrated to recognize sialic acid (SA) on the cell surface. Under optimal conditions, the impedimetric cytosensor exhibited a good linear relationship with the logarithm of the cell concentration from 17 to 1.7×10^6 cells mL^{-1}, and the low detection limit was 6 cells mL^{-1} (S/N=3). Therefore, the electrochemical impedimetric biosensor offers a potential approach to bedside rapid detection of RCC in clinical applications.

Keywords: 3-aminophenyl boronic acid; PPy-Ag@BSA; impedimetric cytosensor;

[1] Chao Yu and Lei Zhang contributed equally to this work.

sialic acid; renal cell carcinoma.

1. Introduction

Renal cell carcinoma (RCC) accounts for 2%-3% of adult malignant tumours. In the world, more than 200,000 new cases and more than 100,000 mortality events occur every year due to RCC (Zou et al. 2014). Various techniques for RCC early diagnosis have been reported, such as western blotting(Argani et al. 2010), immunohistochemistry (Rao et al. 2016; Song et al. 2015; Yeh et al. 2015), and reverse transcription polymerase chain reaction (RT-PCR) (Jin et al. 2014). However, these methods are costly, time-consuming and complex, and require strict laboratory conditions, and certain processes have unsatisfactory specificity and sensitivity (Cho et al. 2015). All of these drawbacks greatly limit the application of these techniques. Approximately 1/3 of RCC patients are metastatic at the time of diagnosis using traditional methods (Brookman-May et al. 2013). Compared with traditional methods, cell biosensors have attracted heightened attention because of their simplicity, rapidity and low cost. Furthermore, cell biosensors are highly sensitive with low cytotoxicity and do not require sophisticated instruments. To the best of our knowledge, no reports are available on cell-based electrochemical detection of kidney cancer cells. Thus, the development of a highly sensitive and selective cell-based electrochemical sensor for kidney cancer diagnosis is urgently needed.

Sialic acid (SA), a monosaccharide with a nine-carbon backbone, is a component of oligosaccharide chains in mucins, glycoproteins and glycolipids that occupies the terminal non-reducing positions of complex carbohydrates on both external and internal membrane areas where they are highly exposed and develop important functions (Liu et al. 2013; Matsumoto et al. 2009). Metastatic cancer cells often express a high density of sialic acid-rich glycoproteins. Because over-expression of sialic acid on the cell surface creates a negative charge on the cell membranes, it results in repulsion between cells and helps these late-stage cancer cells enter the blood stream or urine (Fuster and Esko 2005). The amount of sialic acid increases sharply with the deterioration of the tumour (Qian et al. 2012; Zhang et al. 2010). Thus, monitoring the expression level of sialic acid on the cell surface is of great significance for the diagnosis and treatment of cancers. In this work, we propose the

use of an electrochemical impedimetric cytosensor for the detection of kidney cancer cells in human urine using sialic acid-rich glycoproteins on the cell surface.

Maintaining the original cell condition should be taken into consideration in the cytosensor as avoiding the interaction between cell compositions and toxic materials. So the identification of a low cytotoxicity biomaterial with excellent electrical-conductivity is of great importance. (Cai et al. 2015; Zhang et al. 2015). Polypyrrole (PPy) is a typical organic conducting polymer, that has been widely used as a substrate material because of its high electrical conductivity, chemical stability and low cytotoxicity (Li et al. 2015; Mao et al. 2015; Marks et al. 2002). Moreover, PPy possesses excellent biocompatibility, a large surface area and a unique construction that facilitates its binding to a variety of other biomolecules (Rong et al. 2015; Zhang et al. 2015). Additionally, PPy has a strong background current and affects the process of experiment due to the conjugated system of bonds and the coplanar arrangement of the electrodes (Jin et al. 2016; Xiao et al. 2007). However, the protein complexes could weaken the background current which results from PPy. Ag@BSA, a 3D protein-inorganic composite, possesses an open nanoporous structure, excellent biological properties and a large surface area (Cao et al. 2015; Hu et al. 2013; Hu et al. 2012). In addition, the outer BSA molecules can block nonspecific sites and reduce nonspecific interactions between Ag microspheres and their targets (Cozzi 2004). Thus, Ag@BSA is expected to serve as a highly useful material for the fabrication of cell biosensors. In this study, the PPy-Ag@BSA film was electrochemically co-deposited onto the surface of a gold electrode. PPy-Ag@BSA film has the common advantages of PPy and Ag@BSA, which could enlarge the surface of electrode and capture more APBA molecules by cross-linker. Meanwhile, it could enhance the cytosensor's sensitivity and biocompatibility. Furthermore, the copolymerization was proposed for the first time as a cell biosensor with its simplified procedure.

To quickly capture living cells, 3-aminophenylboronic acid (APBA), a borate compound, was chosen as a capture probe. APBA molecules are able to stably bind with the 1, 2- or 1, 3-diols of carbohydrate chains in aqueous milieu, particularly at

physiological pH 7.4 (Qian et al. 2012). Compared with other carbohydrates (mannose, galactose, etc.), APBA has higher specific binding capacity for SA. In this study, we focused on the APBA interaction with SA on the cell membrane and obtained a much lower detection limit of cancer cells than in previous work (Ellis et al. 2012; Han et al. 2011; Huang et al. 2014; Otsuka et al. 2003). Additionally, PDITC was selected as the cross-linking agent in this work. PDITC has been used as a drug for the treatment of cancer, parasitic diseases and in a few applications in the biosensing field (Elshafey et al. 2013). PDITC has a lower toxicity and better conductive properties than glutaradehyde (GA), and the cytotoxicity of this method is lower than that shown in the existing literature (Cao et al. 2015).

This paper demonstrates a direct, minimally cytotoxic and highly selective electrochemical cell biosensing method using an impedimetric biosensor modified with a PPy-Ag@BSA film. To the best of our knowledge, this is the first report of the application of a PPy-Ag@BSA SP film in a cell biosensor. In addition, a new micromolecule probe of APBA was applied. With these materials applied, the sensitivity of the cytosensor was significantly improved. Moreover, this study demonstrates the first electrochemical detection of metastatic cancer cells.

2. Experimental

2.1. Materials and reagents

Pyrrole (98%), 3-aminophenylboronic acid monohydrate (APBA) and bovine serum albumin (BSA) were purchased from Sigma-Aldrich (St. Louis, USA, www.sigmaadrich.com). Ascorbic acid ($C_6H_6O_8$), sodium dodecyl sulphate (SDS), silver nitrate ($AgNO_3$), KCl (>98%), potassium ferrocyanide [$K_4Fe(CN)_6$] and potassium ferricyanide [$K_3Fe(CN)_6$]were ordered from Sigma-Aldrich (Beijing, China). Cell Counting Kit-8 (CCK-8) and sialic acid (SA) were obtained from Dojindo (Shanghai, China). Phosphate buffer solutions (PBS) (pH 7.4) were prepared with Na_2HPO_4 and KH_2PO_4. Other chemical reagents were of analytical grade and

used without further purification. All solutions were prepared with de-ionized water (> 18 MΩ cm) from a Milli-Q system.

2.2. Apparatus and measurements

The morphologies of the materials were characterized using scanning electron microscopy (SEM, Hitachi S-3000N, Japan), X-ray diffraction (XRD, Y-2000, Dandong oron ray instrument co., Ltd, China), FT-IR spectrometry (Nicolet 6700, Thermo Nicolet, USA) and transmission electron microscopy (TEM, Hitachi-7500158, Japan) as well as 3D laser microscopy (Keyence, Shanghai). Energy dispersive X-ray spectroscopy (EDS) was performed with a JEOL JSM-6700F microscope (Japan). Electrochemical measurements, including cyclic voltammetry (CV), electrochemical impedance spectroscopy (EIS) and differential pulse voltammetry (DPV), were performed on a CHI 660E workstation at room temperature with a three-electrode system containing a reference electrode (saturated calomel electrode), a counter electrode (0.5-mm diameter platinum wire) and a working electrode (4-mm diameter gold electrode) (Chenhua Instruments Co., Shanghai, China). All electrochemical experiments were performed in a 5 mM $[Fe(CN)_6]^{3-/4-}$ solution containing 0.1 M KCl.

2.3. Cell culture and collection

Cell culture and collection are described in the Supplementary Information (S1.1).

2.4. Synthesis of Ag@BSA submicron particles

Synthesis of Ag@BSA submicron particles is described in the Supplementary Information (S1.2).

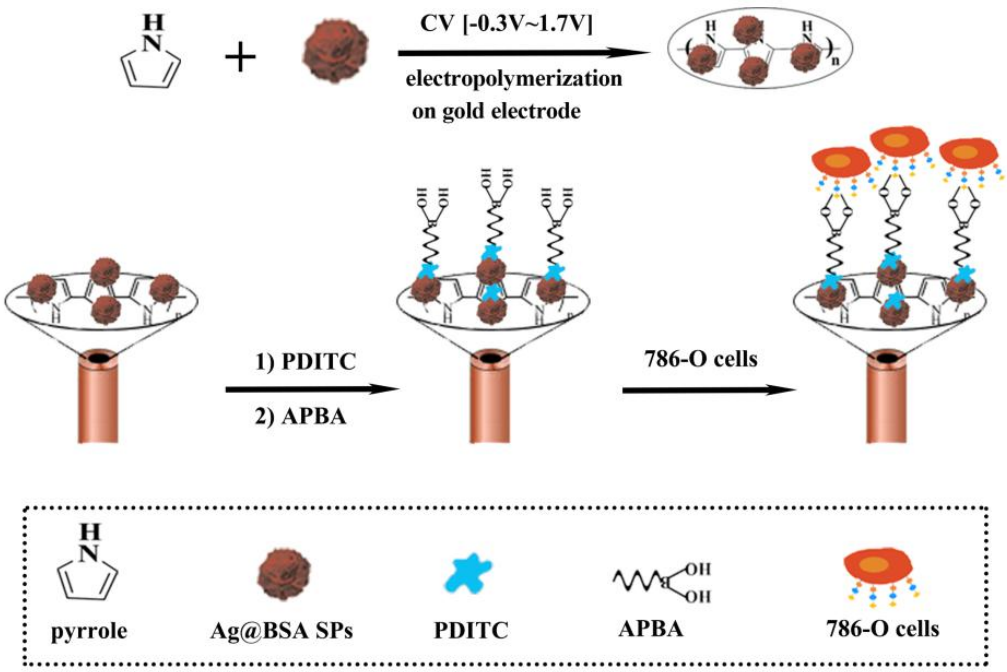

Scheme 1. Schematic representation of the electrochemical impedimetric cytosensor.

2.5. CCK-8 assays

The cytotoxicity of the material in *vitro* was measured using a CCK-8 assay. Initially, 786-O cells at a density of 10000 cells/well were cultured for 24 h and 48 h in 96-well plates in RPMI 1640 medium with 10% FBS in a humidified environment containing 5% CO_2 at 37 °C. Subsequently, the medium was substituted with fresh medium supplemented with various concentrations of Ag@BSA submicron particles (0.1, 0.2, 0.3, 0.4, 0.5, 1 mg mL^{-1}). Each concentration was tested in 3 wells. After 24 h and 48 h, the modified electrode was washed with PBS (pH 7.4) three times and cultured in medium with CCK-8 (v/v, 1:10) at 37 °C in an incubator for 4 h. Finally, the absorbance of each well was measured using a microplate reader at 490 nm until the color of the medium did not change significantly. Cell viability was measured according to the following formula:

$$\text{Cell viability (\%)} = \frac{(\text{As} - \text{Ab})}{(\text{Ac} - \text{Ab})} \times 100\%.$$

As, Ab and Ac represent the values of the experiment group, blank group and control group, respectively. The control group was seeded with target cells, the experiment group was incubated with the addition of biomaterials under the same conditions, and the blank group only included medium.

2.6. *Electropolymerization of the PPy-Ag@BSA film on gold electrodes*

The PPy-Ag@BSA film was synthesized with CV technique, as previously reported with a minor modification (Xiao et al. 2007). Herein, a gold electrode (GE, 4.0-mm diameter) was chosen as a working electrode for modification. Prior to modification, the GE was polished with 0.3 and 0.05 μm α-alumina powder to form a mirror-like surface, followed by sonication with ultrapure water and ethanol to remove residuals. Then, the GE was allowed to dry with nitrogen at room temperature. Thereafter, the mixture solution included 0.1 M pyrrole monomer, 0.5 mg mL^{-1} Ag@BSA and 0.02 M SDS, and was blown with nitrogen for 5 min before use. SDS was used as a dopant and helped to form the composite layer. Successively, electrochemical copolymerization was performed with 15 cycles using a CV technique with a scan rate of 20 mV s^{-1} and a voltage range from -0.3 V to +1.7 V. The modified electrode with PPy-Ag@BSA film was dried with nitrogen and preserved at 4 °C. In the course of the electro-polymerization, reproducibility was very good because the thickness of the film, one of the important parameters for cytosensor, could be very well controlled via the CV technique.

2.7. Fabrication of the electrochemical cytosensor

The fabrication procedure of the electrochemical cytosensor is illustrated in Scheme 1. On the surface of the PPy-Ag@BSA modified electrode, PDITC (6 μL, 1.5 mM), a "green" and low toxicity cross-linker, was incubated for approximately 60 min to form the interaction between the thiocyanate groups on PDITC and the amino groups of Ag@BSA. An APBA solution (6 μL, 0.46 mM) was added to the surface of

the PDITC-modified electrode and incubated for 60 min at room temperature. After each step of biosensor construction, the modified electrode was washed with PBS buffer (pH 7.4) three times to eliminate residues that were not bonded onto the surface. Before cell detection, the modified biosensor was stored at 4 °C without any buffer.

2.8. Detection of 786-O cells

To guarantee an optimal cell physiological environment, 786-O cells were collected and suspended in PBS buffer (pH 7.4). The concentrations of target cells were counted using trypan blue and Cedex XS system. Various concentrations of 786-O cells ranging from 17 to1.7× 10^6 cells mL^{-1} were measured. After incubation for 60 min, the biosensor was washed with PBS (pH 7.4) to eliminate the unlinked cells.

3. Results and discussion

3.1. Morphology and characterization of Ag@BSA submicron particles

Ag@BSA submicron particles play a significant role in the fabrication of the sensitive electrochemical cytosensor. Fig. 1A and B showed the SEM images of Ag microspheres (AgMSs) and Ag@BSA, AgMSs displayed a ball-like structure with an average diameter of 1 μm approximately. Compared with the structure of AgMSs, Ag@BSA revealed a flower-like submicron structure with an average diameter of 3 μm and a good monodispersity, which was beneficial to develop a homogeneous film. The preliminary results indicated the significant difference between Ag@BSA and AgMSs. According to Fig. 1C and D, a porous flower morphology coated with a thin film of BSA molecules was displayed in the TEM images at different magnifications, and this morphology was consistent with previous reports (Cao et al. 2015). Herein, innumerable tiny AgMSs enhanced the sensitivity of the proposed cytosensor by promoting electron transfer. The external layer (BSA) could conjugate more targeting

molecules using the amino groups and was employed as an ideal sealing agent to block nonspecific sites.

As shown in Fig. 1E, FT-IR spectroscopy revealed the primary functional groups of Ag@BSA. A broad absorption peak was displayed at 3281 cm^{-1}, indicating combination of the N-H and O-H stretching vibrations of BSA. These groups forced the BSA-incorporated Ag nanoflowers to disperse homogeneously in PBS or water. The relatively weak peak at 2160 cm^{-1} corresponded to the H-S bond from BSA. An obvious absorption peak was observed at 1390 cm^{-1}, which suggested the wagging vibrations of the $-CH_2$ groups in BSA. The bands for the amide I groups of the protein at 1610-1690 cm^{-1} were consistent with the C=O stretching vibration of peptide linkages, and the amide II groups at 1500-1600 cm^{-1} denoted a combination of N-H bending and C-N stretching, leading to two absorption peaks at 1640 cm^{-1} and 1530 cm^{-1}. Therefore, the observed absorption bands confirmed the preservation of BSA molecules. In addition, the EDS response of the Ag@BSA could be observed in Fig. 1F. Significant peaks for C, N, O and Ag were obtained, indicating that Ag@BSA was successfully synthesized.

To obtain an excellent electrochemical cytosensor, the biomaterials used as a substrate must be involved the electron conductivity and must also be probed for their cytotoxicity. CCK-8 assays were performed to evaluate the cytotoxicity of the nanoflowers at various concentrations in a 37 °C incubator for 24 h and 48 h (Fig. S1). The diagram showed that the viability of 786-O cells was not significantly different compared to that for the controls. More than 90% of 786-Ocells were still alive at a concentration of 0.1 to 0.5 mg mL^{-1} and even at 1.0 mg mL^{-1} with only a slight change. Thus, the excellent biocompatibility of Ag@BSA was further confirmed.

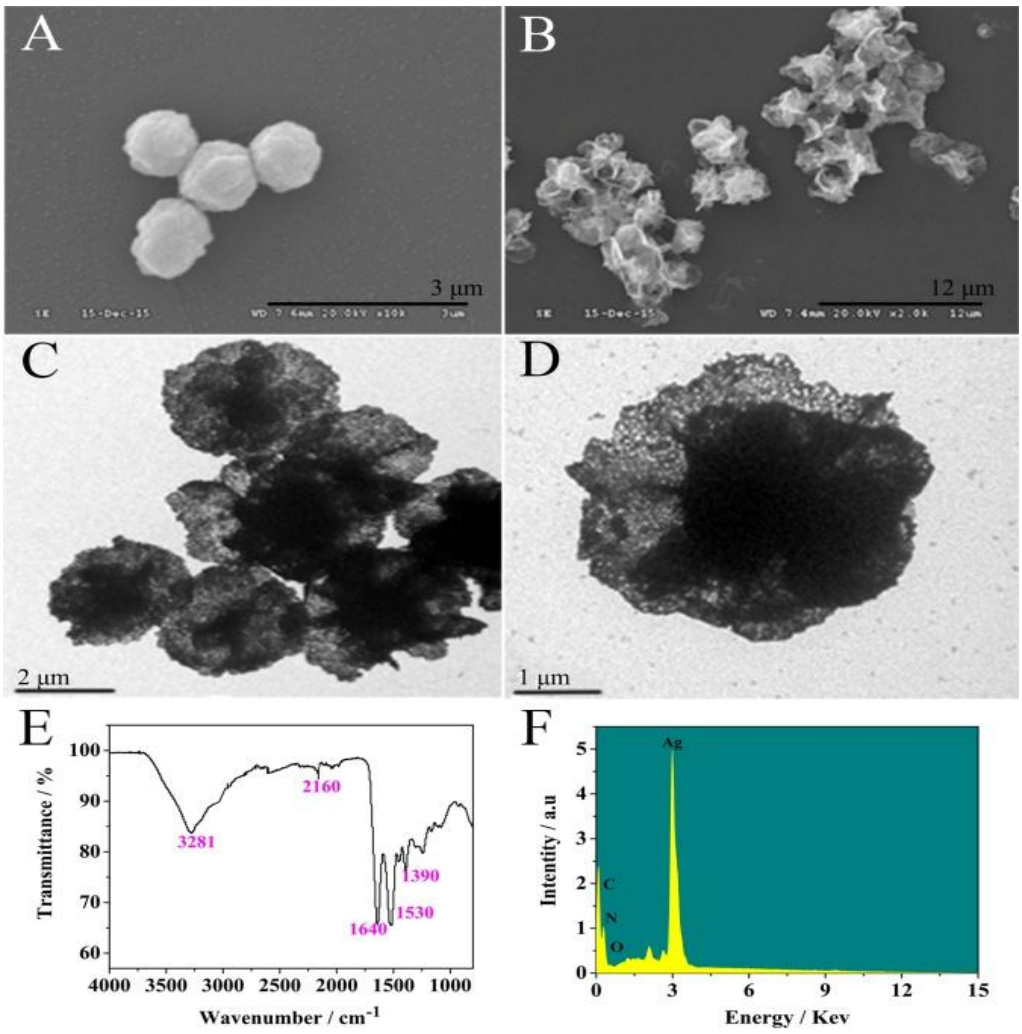

Fig. 1. SEM images of AgMSs (A) and Ag@BSA (B). TEM (C, D) images of Ag@BSA from lower magnification to higher magnification. FT-IR spectrum (E) and EDS (F) of Ag@BSA.

3.2. Characterization of the PPy-Ag@BSA composite

A good sensing film has a pivotal impact on the performance of a cytosensor. PPy-Ag@BSA film was acted as a multifunctional platform and improved the cytosensor's sensitivity and biocompatibility. In order to confirm the successful polymerization of PPy-Ag@BSA film, PPy film and PPy-Ag@BSA layer were characterized with SEM (Fig. 2A, B,), 3D laser scanning microscopy (Fig. 2C, D, E)

and XRD (Fig. 2F). Fig. 2A showed that the PPy film had a rough cauliflower-like structure and morphology. Because the PPy film had a large surface area and a good biocompatibility, it promoted electron transfer and was modified with more biomolecules. Compared with the PPy film, the PPy-Ag@BSA layer displayed a flat morphology in Fig. 2B, indicating that this layer had been successfully prepared. At the same time, 3D laser scanning microscopy images showed that the roughness of the unmodified PPy film was 4.6 μm and the roughness of the PPy-Ag@BSA layer (2.3 μm) was lower than before the one-step copolymerization (Fig. 2C, D). Therefore, this result further confirmed that PPy-Ag@BSA film was successfully obtained. The PPy-Ag@BSA film provided a large capacity for biomolecules immobilization and a facile pathway for electron transfer. Additionally, the roughness was 14.6μm after incubation of 786-O cells on the modified sensor (Fig. 2E), indicating that this cytosensor had an excellent cell capture ability.

The XRD pattern also confirmed the successful polymerization of the PPy-Ag@BSA (Fig. 2F). According to the literature (Huang et al. 2010; Wan et al. 2008; Wei et al. 2009)，the broad peak appearing at 2θ value of 24º was attributed to the amorphous PPy. In addition, five characteristic peaks of Ag corresponding to Bragg's reflections form (111) (200) (220) (311) (222) crystal faces were observed at 38º, 44º, 64º, 77º and 81º. The result indicated the presence of Ag and PPy in PPy-Ag@BSA composite. Meanwhile, CV was also utilized to investigate the conductivity of the PPy film (curve a) and the PPy-Ag@BSA layer (curve b) (Fig. S4.). The PPy film had strong background current resulting from the coplanar arrangement of the electrodes, but Ag@BSA reduced the background current due to the existence of BSA. Thus, the peak current of the PPy film was higher than curve b and the change current achieved was 441 μA. All of the results demonstrated that the PPy-Ag@BSA sensing film was successfully synthesized.

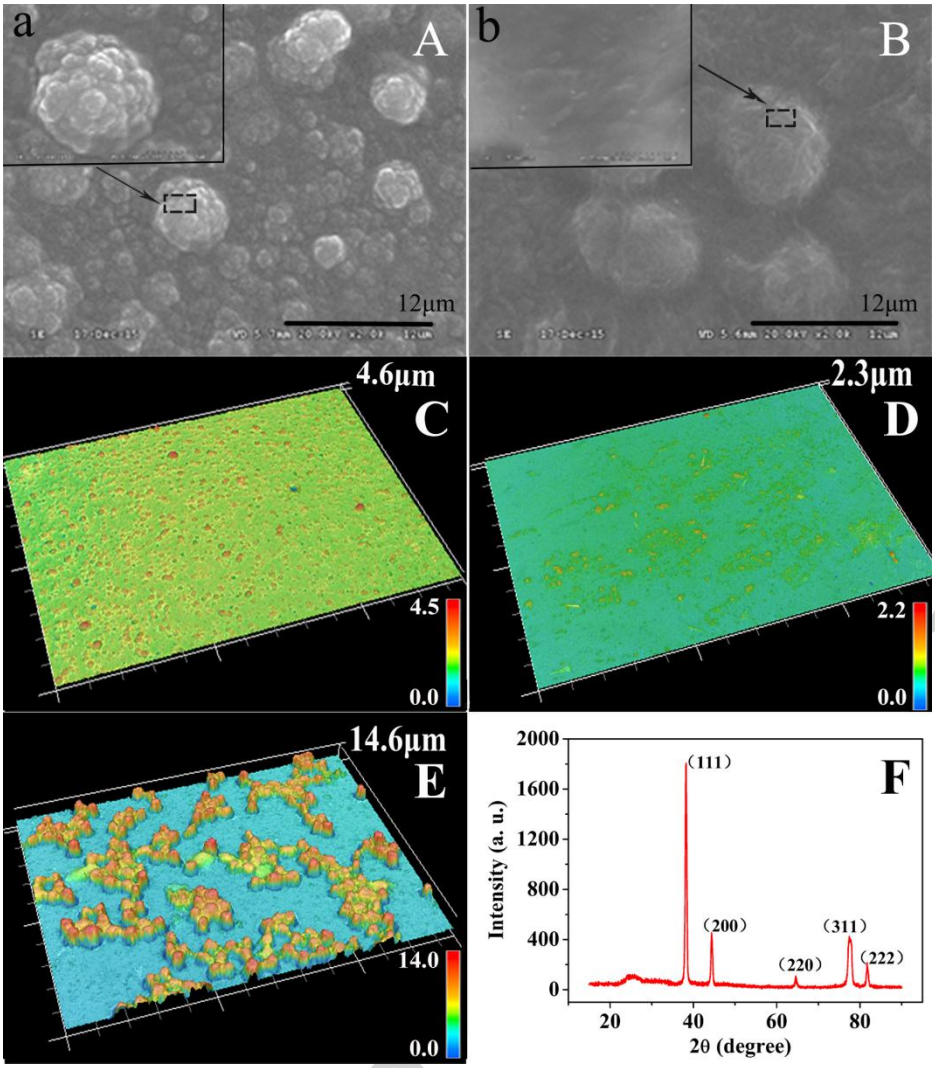

Fig. 2. SEM images of (A) PPy and (B) PPy-Ag@BSA sensing films. The inset shows the morphology of the PPy and PPy-Ag@BSA films at higher magnification. 3D laser scanning images of (C) PPy, (D) PPy/BSA-incorporated Ag nanoflowers and (E) PPy-Ag@BSA sensing films after incubation with 786-O cells. (F) The XRD pattern of PPy-Ag@BSA composite in the range of 15º-90º.

3.3. Electrochemical characterization of the cytosensor

EIS and DPV have been popularly applied to monitor the assembly processes of cytosensor, because of their sensitive and immediate responses for electro-active substances. The impedance spectrum consisted of a similar semicircle part at the low

frequency resulting from the electron transfer limited process and a linear portion at high frequency indicative of the diffusion limited electrochemical process. The diameter of the similar semicircle showed the electron transfer resistance of the modified layer and reflected its blocking behavior of the electrode in the real impedance. In impedance analysis, the impedance parameters include a frequency range of 1 x 10^{-1} Hz to 1 x 10^{6} Hz, amplitude of 0.005 and integration time of 102 s. The DPV measurements were employed containing a 20-mV pulse amplitude and a voltage range of -0.1V to +0.5V.

Fig. 3A showed the DPV results of each electrode modification step. First, a standard DPV peak of the bare gold electrode was observed (curve a, 103.0 μA). After the deposition of PPy-Ag@BSA on the electrode surface, the peak current increased markedly (curve b, 123.5 μA), indicating that the PPy-Ag@BSA film could significantly accelerate electron transfer and signal amplification. To conjugate APBA onto the modified film, the PDITC molecule was employed as a "green" cross-linker because its active groups can react with amine groups to form stable functional groups. The current signal clearly decreased after incubation with PDITC molecules (curve c, 89.5 μA), indicating that PDITC was successfully conjugated with the PPy-Ag@BSA film. Subsequently, the peak current further decreased after incubation with the APBA probes (curve d, 64.2 μA), because APBA blocked the electron exchange between the redox probe and the electrode, it indicated that APBA was successfully added to the modified electrode, Finally, based on the high-specific recognition between SA and APBA, 786-O cells (90 cells mL^{-1}) were captured onto the modified electrode surface. The peak current was much lower than before (curve e, 30.7 μA), because a quantity of the target cells was linked to the electrode surface and blocked electron transfer.

Subsequently, EIS was utilized to further confirm fabrication of the cytosensor, and the results were consistent with the DPV results (shown in Fig. 3B). A modified equivalent circuit was employed to fit the impedance spectra on top right corner Fig. 3B. In this inset, this circuit contains the resistance of the electrolyte solution, R_s; the electron transfer resistance, R_{et}; the Warburg impedance, Z_w associated the diffusion process of the redox probe ions to the electrode-solution interface from the bulk of the

electrolyte and the constant phase element CPE which is related to the double layer capacitance. All values that obtained from fitting the experimental data recorded during the cytosensor stepwise fabrication process are displayed in detail in Table S1. These results adequately demonstrated that the proposed impedimetric cytosensor was successfully fabricated.

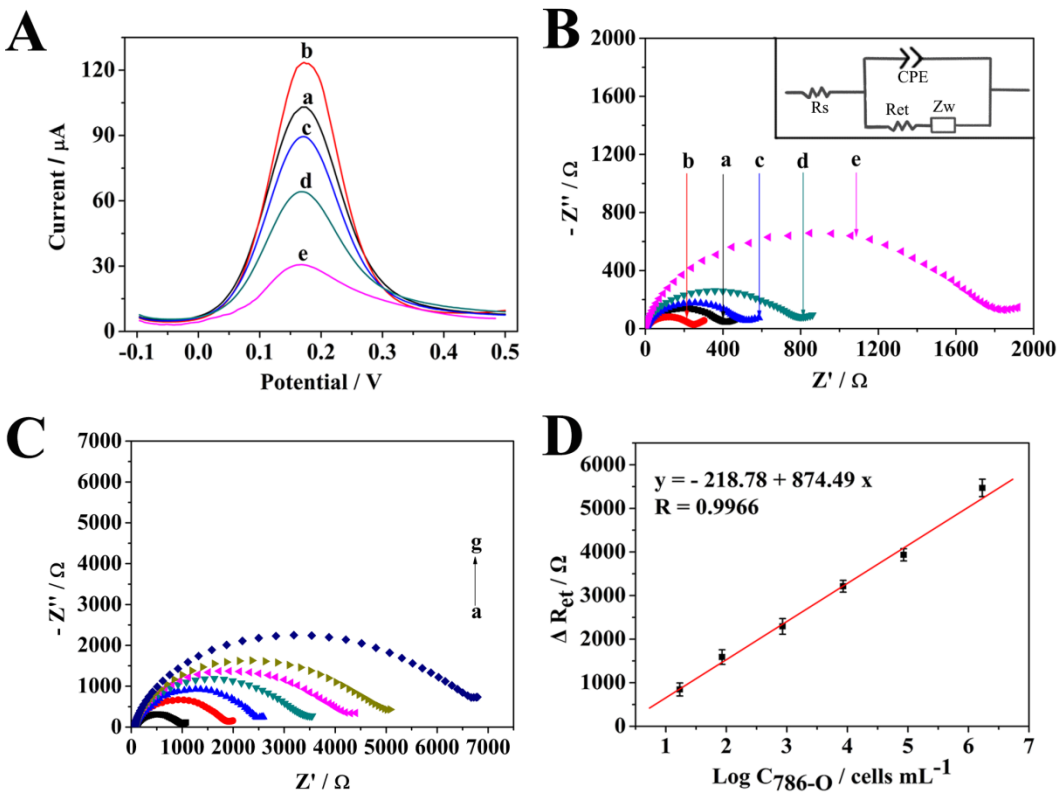

Fig. 3. DPVs (A) and Impedance spectra (B). The experiments were performed in a 5 mM $[Fe(CN)_6]^{3-/4-}$ solution containing 0.1 M KCl: (a) bare GE, (b) PPy-Ag@BSA /GE, (c) PDITC/ PPy-Ag@BSA /GE, (d) APBA/ PDITC/ PPy-Ag@BSA /GE, (e) target cells (90 cells mL^{-1})/ APBA/PDITC/ PPy-Ag@BSA /GE. (C) and (D) response of the cytosensor assay with different concentrations of 786-O cells (0, 17, 85, 8.5×10^2, 8.5×10^3, 8.5×10^4, and 1.7×10^6 cells mL^{-1}). (n=5)

The electrochemical behaviour of the modified electrode surface was further investigated in a 5 mM $[Fe(CN)_6]^{3-/4-}$ solution containing 0.1M KCl. The CVs of the PPy-Ag@BSA modified electrode were displayed at different scan rates in Fig. S3A. The redox peak current increased gradually over the scan rate ranging from 20 to 400

mV s^{-1}. Fig. S3B showed a good linear relationship between the peak currents and the square root of the scan rate. Based on the Randles-Sevcik equation (Li et al. 2015; Muller and Lambert 2011), the results suggested that the redox reaction of the electrode surface was a diffusion-controlled process. In addition, the surface area of the PPy-Ag@BSA-modified electrode was calculated to be 35.74 mm^2, which was approximately triple that of the bare GE.

3.4. Optimization of the experimental conditions

The optimum conditions (the codeposition cycle, APBA incubation time, 786-O cells incubation time) were measured, as shown in Fig. S1. A detailed description can be found in the Supplementary Information (S1.3.)

Table 1 Comparison of the sensitivity of different methods for cell detection.

Brief Biosensing Mechanism	Target Cell	cell incubation time	Linear Range(cell mL^{-1})	LOD (cell mL-1)	Reference
GE/BSA-incorporated Ag nanoflowers/GA/SNA	DLD-1 cell	2 h	1.35×10^2 -1.35×10^7	40	(Cao et al. 2015)
GE/Au@BSA/GA/anti-CEA	BXPC-3	4 h	5.2×10 -5.2×10^7	18	(Hu et al. 2013b)
GCE/Poly-L-lysine	T cell	No present	5.0×10^2 -5.2×10^5	180	(Huang et al. 2014a)
GCE/MWNT/AuNP/SNA	A549 cell	50 min	3.0×10^4-3.0×10^7	700	(Zhang et al. 2010)
GE/Ag@BSA	KB cell	2 h	6.0×10^1-1.2×10^8	20	(Hu et al. 2013a)
GE/PPy-Ag@BSA/PDITC/APBA	786-O cell	1 h	1.7×10-1.7×10^6	6	This work

3.5. Analysis of 786-O cells

EIS was performed with the low frequency range of 1×10^{-1} to 1×10^4 Hz and the high frequency range of 1×10^4 Hz to 1×10^6 Hz to investigate the performance

of the proposed cytosensor and perform quantitative analysis of cancer cells under optimal experimental conditions. In the impedance spectra, the impedance values increased as the diameters of the similar semicircle increase in the real impedance. Fig.3C showed the impedance response of the modified sensor in the absence and presence of various concentrations of 786-O cells. The changes in the size of the semicircle curve clearly suggested an ultrasensitive response signal between the capture probe and different concentrations of cancer cells onto the modified electrode surface. Because of the amounts of specific recognitions, the redox probe's attachment to the sensor surface was gradually hindered. With the concentration of target cells increased, the size of the semicircle curve increased significantly. The analysis results from statistical correlation calculations exhibited a good linear relationship with the logarithm of the target cell concentration in the range of 17 to 1.7×10^6 cells mL^{-1} (Fig. 3D). The linear equation was expressed as:

$$\Delta R_{et}\ (\Omega) = -\ 218.78 + 874.49\ \mathrm{Log}\ C_{786\text{-}O}\ (\text{cells mL}^{-1})$$

The correlation coefficient was 0.9966. Furthermore, the fabricated cytosensor had a lower detection limit than those previous reported (Cao et al. 2015), 6 cells mL^{-1} (S/N = 3). These results indicated that the proposed cytosensor displayed good performance in cancer cell detection. Compared with the other cytosensors (Table 1, Table S2), the proposed biosensor had the lower detection limit and the shorter capture time even if it had no broad linear range, indicating that a sensitive biosensor had been successfully designed. To the best of our knowledge, this is the first study on testing the RCC cells based on impedimetric biosensor. Thus, the cytosensor has better capture capability and excellent sensitivity for the detection of the target tumour cells and is promising in the researches of tumorigenesis process.

3.6. Specificity, stability, and reproducibility of the electrochemical cytosensor

To evaluate the specificity of the biosensor, EIS techniques were used under the

same experimental conditions after incubating the biosensor with leukocytes, epithelial cells, and 786-O cells. As shown in Fig. 4A, compared with the response of biosensor to 1 × 10^4 786-O cells ml^{-1}, the biosensor had no significant response towards leukocytes and epithelial cells. The result suggested that this biosensor had good selectivity for target cells.

The long term stability of this cell biosensor was probed. The APBA/PDITC/PPy-Ag@BSA modified cytosensor was stored at 4 °C in a refrigerator for 7d, 14d, and 28d, and the response signal remained were 93.4%, 91.53%, and 85.61% of the initial response, respectively. The results indicated that the developed cytosensor displayed excellent stability.

The reproducibility of the cytosensor also plays an important role in clinical detection. Five modified electrodes were tested with the target cancer cells (1.0 × 10^4 cells ml^{-1}), and the average value of the relative standard deviation (RSD) was 3.9%, suggesting that the developed cytosensor showed good reproducibility.

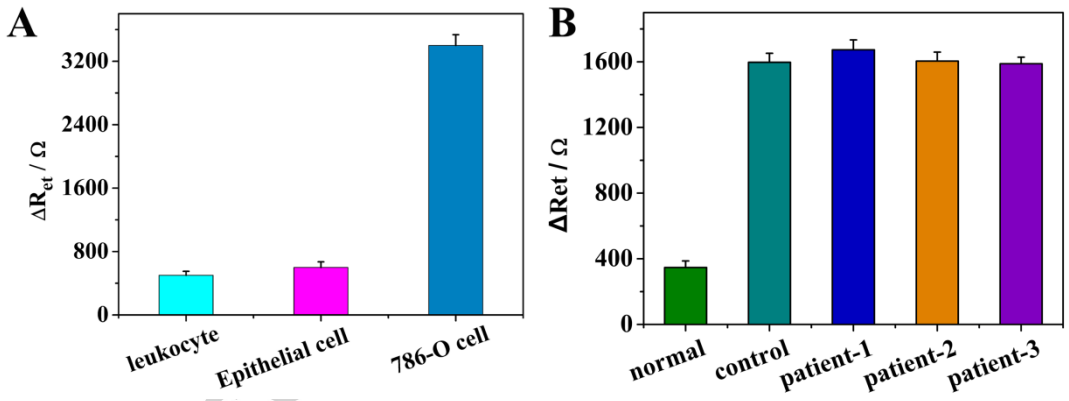

Fig. 4. EIS response after incubation with the same concentration of leukocytes, epithelial cells, and 786-O cells (A). Analysis of patients' urine samples, control and normal urine samples (B) in a 5 mM $[Fe(CN)_6]^{3-/4-}$ solution containing 0.1 M KCl.(n=3)

3.7. Application in human urine samples

To investigate the application of the proposed impedance cytosensor to real samples, urine samples from three kidney cancer patients and one healthy person were

collected and analysed under optimal conditions. Meanwhile, we re-suspended the 786-O cells in the health urine as the false positive control. This control would rule out that the urine of the patients has some other component that might give false positive results. The urine samples were suspended in PBS (pH 7.4) after centrifugation. Each urine sample except for the normal included approximately 1.0×10^2 cells ml^{-1} and was measured 3 times using the proposed biosensor. As shown in Fig. 4B, the patient groups were not significantly different from each other, but the ΔR_{et} of the patient groups changed sharply compared with that of the normal group. Furthermore, the RSD between the control and the patients was 2.407%. As a result, the modified cytosensor was able to distinctly differentiate between normal and abnormal samples and achieved the RCC diagnosis in clinical samples.

4. Conclusions

In this work, we have successfully designed a facile and non-invasive electrochemical cytosensing strategy for rapid detection of RCC via specific recognition between APBA and SA on the cell membrane. The advantages of the developed cytosensor are as follows: (1) The gold electrode was firstly modified with PPy-Ag@BSA performed as a splendid sensing film for cell adhesion study, due to its excellent biocompatibility, conductivity and convenient synthesis route. (2) With the help of APBA, a much lower detection limit and a higher specificity have been achieved by this method. (3) Non-invasive diagnosis of RCC has been achieved using urine samples of patients. This cytosensor with rapid response from EIS and simple operation may provide a promising approach for cell-based diagnosis and lead to the development of a new diagnostic tool for RCC.

Acknowledgments

This research was supported financially by the National Natural Science Foundation of China (No. 81370403, 31571554), the Chongqing foundation and advanced research project (No. CSTC2015jcyjBX0053), and the Chongqing medical

university scientific research cultivating fund (No.201414).

References

Argani, P., Hicks, J., De Marzo, A.M., Albadine, R., Illei, P.B., Ladanyi, M., Reuter, V.E., Netto, G.J., 2010. Am. J. Surg. Pathol 34(9), 1295-1303.

Brookman-May, S.D., May, M., Shariat, S.F., Novara, G., Zigeuner, R., Cindolo, L., De Cobelli, O., De Nunzio, C., Pahernik, S., Wirth, M.P., Longo, N., Simonato, A., Serni, S., Siracusano, S., Volpe, A., Morgia, G., Bertini, R., Dalpiaz, O., Stief, C., Ficarra, V., Members of the, C.-P., Members of the, S.-P., Young Academic Urologists Renal Cancer, G., 2013. BJU. Int. 112(7), 909-916.

Cai, H.H., Pi, J., Lin, X., Li, B., Li, A., Yang, P.H., Cai, J., 2015. Biosens. Bioelectron. 74, 165-169.

Cao, H., Yang, D.P., Ye, D., Zhang, X., Fang, X., Zhang, S., Liu, B., Kong, J., 2015. Biosens. Bioelectron. 68, 329-335.

Cho, M.C., Cho, S.Y., Yoon, C.Y., Lee, S.B., Kwak, C., Kim, H.H., Jeong, H., 2015. PLoS One 10(7), e0130975.

Cozzi, P.G., 2004. Chem. Soc. Rev. 33(7), 410-421.

Ellis, G.A., Palte, M.J., Raines, R.T., 2012. J. Am. Chem. Soc. 134(8), 3631-3634.

Elshafey, R., Tlili, C., Abulrob, A., Tavares, A.C., Zourob, M., 2013. Biosens. Bioelectron. 39(1), 220-225.

Fuster, M.M., Esko, J.D., 2005. Nat. Re.v Cancer 5(7), 526-542.

Han, E., Ding, L., Ju, H., 2011. Anal. Chem. 83(18), 7006-7012.

Hu, C., Yang, D.P., Wang, Z., Huang, P., Wang, X., Chen, D., Cui, D., Yang, M., Jia, N., 2013. Biosens. Bioelectron. 41, 656-662.

Hu, C., Yang, D.P., Xu, K., Cao, H., Wu, B., Cui, D., Jia, N., 2012. Anal. Chem. 84(23), 10324-10331.

Huang, L.L., Jin, Y.J., Zhao, D., Yu, C., Hao, J., Xie, H.Y., 2014. Anal. Bioanal. Chem. 406(11), 2687-2693.

Huang, P., Li, Z., Hu, H., Cui, D., 2010. Journal of Nanomaterials 2010, 1-6.

Jin, B., Gao, F., Zhu, Y.F., Lang, X.Y., Han, G.F., Gao, W., Wen, Z., Zhao, M., Li, J.C.,

Jiang, Q., 2016. Sci. Rep. 6, 19317.

Jin, W., Cheng, Y.F., Mao, S.Y., Zhu, W.Y., 2014. BMC Microbiol. 14, 104.

Li, Y., He, J., Xia, C., Gao, L., Yu, C., 2015. Biosens. Bioelectron. 70, 392-397.

Liu, J., Qin, Y., Li, D., Wang, T., Liu, Y., Wang, J., Wang, E., 2013. Biosens. Bioelectron. 41, 436-441.

Mao, H., Liang, J., Zhang, H., Pei, Q., Liu, D., Wu, S., Zhang, Y., Song, X.M., 2015. Biosens. Bioelectron. 70, 289-298.

Marks, R.S., Novoa, A., Thomassey, D., Cosnier, S., 2002. Anal. Bioanal. Chem. 374(6), 1056-1063.

Matsumoto, A., Sato, N., Kataoka, K., Miyahara, Y., 2009. J. Am. Chem. Soc. 131(34), 12022-12023.

Muller, C.I., Lambert, C., 2011. Langmuir 27(8), 5029-5039.

Otsuka, H., Uchimura, E., Koshino, H., Okano, T., Kataoka, K., 2003. J. Am. Chem. Soc. 125(12), 3493-3502.

Qian, R., Ding, L., Bao, L., He, S., Ju, H., 2012. Chem. Commun. 48(32), 3848-3850.

Rao, Q., Xia, Q.Y., Cheng, L., Zhou, X.J., 2016. Chin. J. Cancer Res. 28(1), 29-49.

Rong, Q., Han, H., Feng, F., Ma, Z., 2015. Sci. Rep. 5, 11440.

Song, W., Yeh, C.R., He, D., Wang, Y., Xie, H., Pang, S.T., Chang, L.S., Li, L., Yeh, S., 2015. Oncotarget 6(22), 19290-19304.

Wan, A.J., Sun, Y., Li, W.T., Li, H.L., 2008. J. Biomed Mater Res. B. Appl. Biomater 86(1), 197-207.

Wei, Y., Li, L., Yang, X., Pan, G., Yan, G., Yu, X., 2009. Nanoscale Res. Lett. 5(2), 433-437.

Xiao, Y., Li, C.M., Liu, Y., 2007. Biosens. Bioelectron. 22(12), 3161-3166.

Yeh, C.R., Ou, Z.Y., Xiao, G.Q., Guancial, E., Yeh, S., 2015. Oncotarget 6(42), 44346-44359.

Zhang, L., Lei, J., Ma, F., Ling, P., Liu, J., Ju, H., 2015. Chem. Commun. 51(54), 10831-10834.

Zhang, X., Teng, Y., Fu, Y., Xu, L., Zhang, S., He, B., Wang, C., Zhang, W., 2010. Anal. Chem. 82(22), 9455-9460.

Zou, B., Han, Z., Wang, Z., Bian, J., Xu, J., Wang, H., Yang, M., Pei, F., Li, S., Xu, Z., 2014. J Cancer Res. Clin. Oncol. 140(10), 1733-1738.

Highlights:

1. A noninvasive cytosensor for detection of renal cell carcinoma (RCC) in urine samples.
2. 3-aminophenyl boronic acid (APBA) as a capture probe based on the specific interaction between APBA and sialic acid (SA).
3. Polypyrrole (PPy)-Ag@BSA film accelerated the signal amplification of the biosensor.
4. A highly accurate, low detection limit and specific biosensor was used for noninvasive diagnosis.